Analytical Methods

Accepted Manuscript

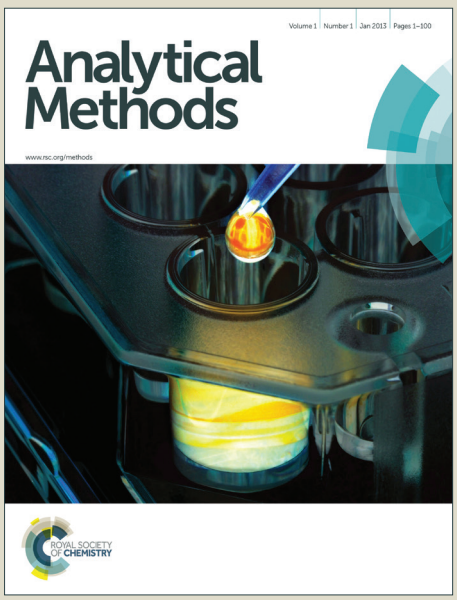

ROYAL SOCIETY OF CHEMISTRY

www.rsc.org/methods

Cite this: DOI: 10.1039/c0xx00000x

www.rsc.org/xxxxxx

ARTICLE TYPE

Simultaneous determination of ascorbic acid, dopamine, uric acid and hydrogen peroxide based on coimmobilization of PEDOT and FAD using multi-walled carbon nanotubes

Kuo Chiang Lin, Jia Yan Huang and Shen Ming Chen*

Received (in XXX, XXX) Xth XXXXXXXXX 20XX, Accepted Xth XXXXXXXXX 20XX
DOI: 10.1039/b000000x

A simple method is used to synthesize the active hybrid composites containing multi-walled carbon nanotubes (MWCNT), 3,4-dioxyetylenethiophene (EDOT), flavin adenine dinucleotide (FAD). The MWCNT/PEDOT-FAD hybrid composite is proposed due to good electrocatalytic properties for ascorbic acid (AA), dopamine (DA), uric acid (UA), and hydrogen peroxide (H_2O_2), after comparing to PEDOT, PEDOT-FAD, MWCNT/PEDOT, and PEDOT-FAD/MWCNT. It shows the linear concentration range of 4×10^{-4} – 8×10^{-3} M, 6×10^{-6} – 7.5×10^{-5} M, 2×10^{-6} – 4×10^{-5} M; the sensitivity of 36 μM mM^{-1} cm^{-2}, 5154 μM mM^{-1} cm^{-2}, and 14286 μM mM^{-1} cm^{-2}; and the detection limit of 4×10^{-4} M, 6×10^{-6} M, and 2×10^{-6} M (S/N= 3) for AA, DA, and UA, respectively. It also shows good electrocatalytic reduction for H_2O_2 with the linear concentration range of 5×10^{-4} – 9×10^{-3} M; the sensitivity of 52 μA mM^{-1} cm^{-2} and detection limit of 5×10^{-4} M (S/N= 3). As the results, it demonstrates a simple method to synthesize the active species on electrode surface for simultaneously determining AA, DA, and UA, as well as H_2O_2. It can be utilized to develop multifunctional biosensors.

1. Introduction

AA, DA, and UA are important biomolecules usually coexist in our body fluids and which play significant roles in the neurotransmission and metabolism of human bodies.[1–3] The levels of AA, DA, and UA can be used to detect some diseases in clinical diagnosis, such as Parkinsonism, HIV infection, leukemia, diabetes, etc. Therefore, it is getting more and more important for the determination of AA, DA, and UA.

The electrochemical technique has received extensive interest in routine analysis, because of its unique superiority such as high sensitivity and fast response on the basis of high electrochemical activity for AA, DA, and UA. However, simultaneous electrochemical determination of these biomolecules at an unmodified electrode results in poor selectivity and low reproducibility, due to overlapping oxidation peaks and electrode fouling, respectively.[4] To solve these problems, considerable efforts have been devoted to improve the electrochemical methods and modify the electrode surface by various carbon materials, including carbon nanofibers,[5,6] anodized nanocrystalline graphite-like pyrolytic carbon,[7] multi-walled carbon nanotubes,[8] graphene,[9,10] single-walled carbon nanohorn[11] and ordered mesoporous carbon.[12] As alternative electrocatalysts, carbon nanotubes (CNTs) including single-walled carbon nanotubes (SWCNT) and MWCNT present excellent performance due to their unique physical, electronic and chemical properties.[13–16] CNTs have been demonstrated to promote electron transfer reaction, which shows superior performance when directly used as electrode materials for analytical applications and diagnostic research purposes.[17–19]

Ulrich et al. have reviewed conducting polymers applied in chemical sensors and arrays.[20] Among the conducting polymers, poly(3,4-ethylendioxythiophene), PEDOT, is a very attractive material due to its low band gap, high conductivity and stability, and transparency in the doped state.[21–23] PEDOT has been proposed as an alternative to traditional polymers as the electroactive component in biosensors.[24,25] When it composed with MWCNT, it shows good sensitivity and selectivity for AA, DA, and UA.[26] It is valuable to keep further researching for application in biosensors development.

Accurate determination of H_2O_2 is extremely important in the field of food industry, pharmaceutical, clinical, industrial and environmental analysis.[27–30] Many techniques have been employed in the determination of H_2O_2, including titrimetry,[31] chromatography,[32] chemiluminescence[33] and electrochemistry.[34] Among these methods, electrochemistry technique based on enzyme-based biosensors has been developed rapidly due to its low cost and high selectivity.[35–38] However, there are some disadvantages of the enzyme-based biosensors, such as instability, critical operating situation, complicated immobilization procedure and limited lifetime.[39] Therefore, a number of studies have been carried out to improve the nonenzymatic sensors with low detection limit and wide respond range. FAD is a flavoprotein coenzyme that plays an important biological role in many oxidoreductases and in reversible redox conversions in biochemical reactions. It consists of the nucleotide adenine, the sugar ribose, and two phosphate groups. FAD and

$FADH_2$ have an isoalloxazine ring as the redoxactive component that readily accepts and donates electrons. This makes it ideally suited to be an intermediate that is cyclically reduced and then re-oxidized by the metabolic reactions. It can be easily to codeposit with some positive electroactive materials due to the static interaction.[40,41] And it also has been reported with good electrocatalytic property for H_2O_2 reduction. It is worthy to study the relative composites for a H_2O_2 sensor without horseradish peroxidase.

In this paper, we report a study to synthesize the hybrid composite of MWCNT, PEDOT, and FAD. These active species composed in different hybrid types are investigated and compared with the electrocatalytic property for AA, DA, UA, and H_2O_2. The relative active one, MWCNT/PEDOT-FAD, is characterized by cyclic voltammetry (CV) and linear sweep voltammetry (LSV). It is investigated for a multifunctional sensor for AA, DA, UA, and H_2O_2.

2. Experimental

2.1 Materials and apparatus

AA, DA, UA, H_2O_2, EDOT monomer and FAD were purchased from Sigma-Aldrich (USA). Multi-walled carbon nanotubes functionalized with amino group (NH_2-MWCNT), which had MWCNT outer diameter of 13 – 18 nm, MWCNT inside diameter of 4 nm, MWCNT length of 1 – 12 μm, and purity of >99 wt%, was purchased from UniRegion Bio-Tech (TW). All other chemicals (Merck) used were of analytical grade (99%). Double distilled deionized water was used to prepare all the solutions. A phosphate buffer solution (PBS) of pH 7 was prepared using Na_2HPO_4 (0.05 mol L^{-1}) and NaH_2PO_4 (0.05 mol L^{-1}).

The pretreatment of MWCNT is using ADVANTEC filter to purify MWCNT. The electrochemical experiments were conducted using a CHI 1205a electrochemical workstation (CH Instruments, USA) with a conventional three-electrode setup using a bare or PEDOT or PEDOT-FAD or PEDOT-FAD/MWCNT or MWCNT/PEDOT-FAD modified electrode as a working electrode, an Ag/AgCl (3 M KCl) reference electrode, and a platinum wire counter electrode. A BAS (Bioanalytical Systems, Inc., USA) glassy carbon electrode (GCE) with a diameter of 0.3 cm was used for all electrochemical experiments. Prior to the modification process, the GCE was well polished with the help of BAS polishing kit and aqueous slurries of alumina powder (0.05 μm), rinsed and ultrasonicated in double distilled deionized water. All potentials reported in this paper were referred to an Ag/AgCl electrode. The buffer solution was completely deaerated using a nitrogen gas atmosphere. The electrochemical cells were kept properly sealed to avoid interference with oxygen from the atmosphere. The composite was electrochemically analysed by CV and LSV.

2.2 Preparation of the PEDOT, PEDOT-FAD, PEDOT-FAD/MWCNT and MWCNT/PEDOT-FAD modified electrodes

The PEDOT and PEDOT-FAD modified electrodes were prepared in pH 1.5 sulphuric acid solutions by CV. The content of the prepared solutions were 0.01 M EDOT monomer or 0.01 M EDOT + 1×10^{-4} M FAD. They were controlled in same scan rate of 0.1 Vs^{-1}, same scan cycles of 20, but different cycling potential range of 0.2 to 1.1 V and -0.4 to 1.1 V for PEDOT and PEDOT-FAD, respectively.

The amino-functionalized MWCNT was used due to its high conductivity, specific geometry, and well dispersion in aqueous solution. It was directly added into aqueous buffer solution and prepared in 1 mg ml^{-1}. This solution was sonicated for 10 min. 10 μl of the solution was drop-casted on a bare or modified electrode. All CNTs used here were amino-functionalized MWCNT and abbreviated in MWCNT for convenient mention.

The PEDOT-FAD/MWCNT and MWCNT/PEDOT-FAD modified electrodes were defined by the use of MWCNT "before" and "after" the electro-codeposition of PEDOT and FAD.

3. Results and discussion

3.1 Electro-codeposition of PEDOT and FAD on bare GCE and MWCNT/GCE

The electro-codeposition of PEDOT and FAD can be easily performed on both bare GCE and MWCNT/GCE. Fig. 1 shows the voltammograms of PEDOT-FAD electro-codeposition using (A) bare GCE and (B) MWCNT/GCE in pH 1.5 H_2SO_4 solution containing 0.01 M EDOT and 1×10^{-4} M FAD. Both of them show well current development with an obvious redox couple at a formal potential of approximate -0.15 V (vs. Ag/AgCl), indicating that FAD can be well deposited on both GCE and MWCNT/GCE. The hybrid film formation is based on the electro-codeposition due to the static interaction between the positively charged PEDOT and the negatively charged FAD. They are also compared with the current response in initial 20 scan cycles. Insets of Fig. 1 show that the current development of PEDOT-FAD formed on MWCNT/GCE is better than that on bare GCE. One can conclude that the PEDOT-FAD can be well codeposited on MWCNT to form the PEDOT-FAD/MWCNT/GCE modified electrode.

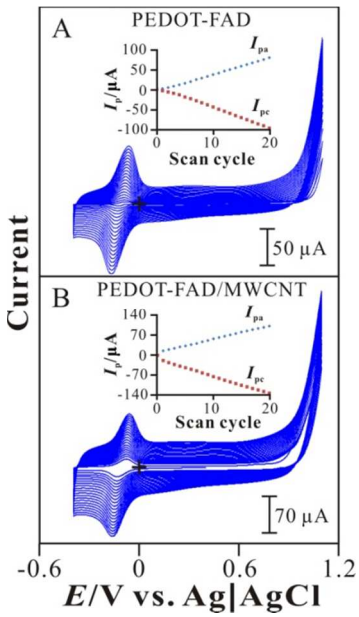

Fig. 1. CVs of (A) GCE and (B) MWCNT/GCE examined in pH 1.5 $H_2SO_{4(aq)}$ containing 1×10^{-2} M EDOT and 1×10^{-4} M FAD. Scan rate = 0.1 V s^{-1}, scan segments = 40. Insets: the plots of

peak current (I_p) vs. scan cycle.

3.2 SEM images and cyclic voltammograms of the different modifiers modified electrodes

Morphology of different modified electrodes was characterized by scanning electron microscopy (SEM). Fig. 2 shows SEM images of (A) PEDOT, (B) PEDOT-FAD, (C) PEDOT-FAD/MWCNT, and (D) MWCNT/PEDOT-FAD modified ITO electrodes. These modified electrodes exhibit globular shape except of MWCNT/PEDOT-FAD. By comparison, the MWCNT/PEDOT-FAD exhibits more flat and uniform structure. This result indicates that the hybrid composites might be more compact and stable in the electrochemical system. One can know that the location of MWCNT after the electro-codeposition of PEDOT and FAD would be more compact in the hybrid composite.

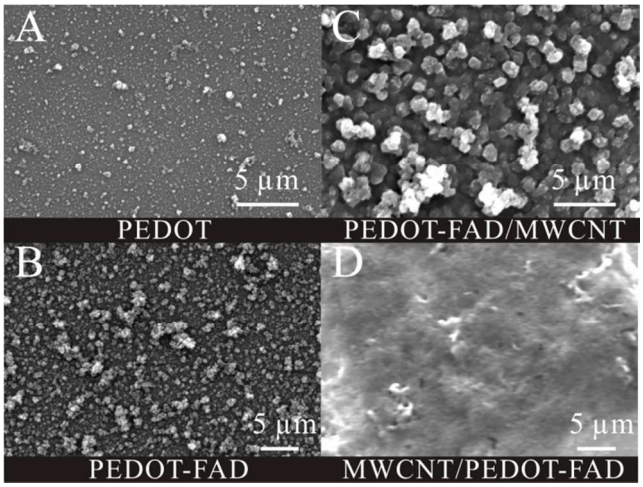

Fig. 2. SEM images of (A) PEDOT, (B) PEDOT-FAD, (C) PEDOT-FAD/MWCNT, and (D) PEDOT-FAD/MWCNT modified ITO electrodes.

To confirm the hybrid film was successfully immobilized on the electrode surface, it was transferred to pH 7 PBS for further study. By the way, the electrochemical response of the relative modifiers was also investigated.

Fig. 3 shows the cyclic voltammograms of different modifiers including PEDOT, MWCNT/PEDOT, PEDOT-FAD, MWCNT/PEDOT-FAD, and MWCNT/PEDOT-FAD. They were examined in blank solution and compared in the potential range from -0.2 V to -0.6 V. PEDOT-FAD, MWCNT/PEDOT-FAD, and PEDOT-FAD/MWCNT (cure c to e) show an obvious redox couple at formal potential $E^{0'}$ = -0.45 V, -0.45 V, and -0.42 V; with peak-to-peak separation (ΔE) of -0.07 V, -0.08 V, and -0.06 V, respectively. The similar formal potential and small separation potential is related to quasi-reversible FAD redox couple involving two-proton and two-electron transfer processes. One can confirm that FAD is well immobilized in these hybrid composites. Moreover, PEDOT-FAD/MWCNT (curve e) shows higher current response and smaller separation potential, suggesting an ideal composite type. In order to confirm this point, PEDOT-FAD, MWCNT/PEDOT-FAD, and PEDOT-FAD/MWCNT were further testing with various scan rates.

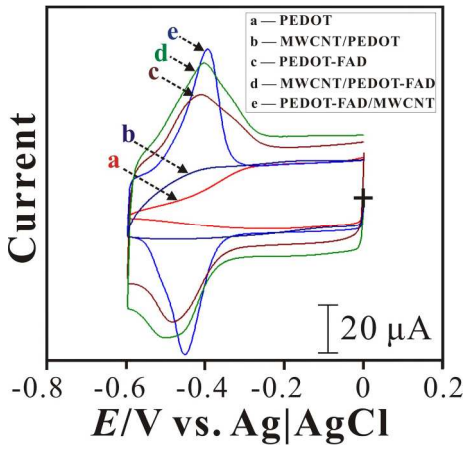

Fig. 3. CVs of (a) PEDOT/GCE, (b) MWCNT/PEDOT/GCE, (c) PEDOT-FAD/GCE, (d) MWCNT/PEDOT-FAD/GCE, and (e) PEDOT-FAD/MWCNT/GCE examined in pH 7 PBS. Scan rate = 0.1 V s^{-1}.

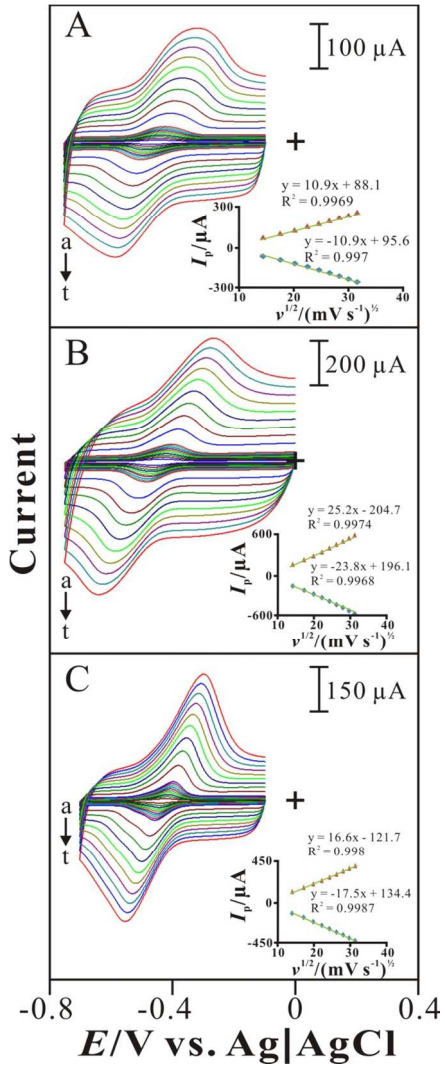

Fig. 4. CVs of (A) PEDOT-FAD/GCE, (B) PEDOT-FAD/MWCNT/GCE, and (C) MWCNT/PEDOT-FAD/GCE examined in pH 7 PBS with various scan rate of 10–1000 mV s^{-1} (a–t). Insets: the plots of peak current (I_p) vs. square root of scan rate ($v^{1/2}$) for case (A), (B), and (C), respectively.

3.3 Cyclic voltammograms of MWCNT/PEDOT-FAD film with various scan rates

Fig. 4 shows the voltammograms of these hybrid composites examined with various scan rates ranging from 10 to 1000 mVs^{-1}. Both anodic and cathodic peak currents are directly proportional to scan rate (v) before 100 mVs^{-1}. After scan rate 100 mVs^{-1}, it is proportional to square root of scan rate ($v^{1/2}$) for these hybrid composites. It indicates that all of them are involving diffusion-controlled processes when scanning in high scan rate. Furthermore, the redox peak shifts were observed and the change between 10 mVs^{-1} and 1000 mVs^{-1} was considered. They were estimated in ΔE_{pa} = 0.071 V, 0.165 V, 0.124 V; and ΔE_{pc} = 0.108 V, 0.179 V, 0.117 V for PEDOT-FAD, MWCNT/PEDOT-FAD, and PEDOT-FAD/MWCNT, respectively. It is obviously seen that PEDOT-FAD/MWCNT has larger peak change. This phenomenon indicates that diffusion effect is getting seriously when MWCNT is first immobilized on electrode surface for the hybrid composite. And the result might provide the important information for preparing the relative hybrid composites in the literature.

3.4 Electrocatalytic oxidation of AA, DA, UA, and electrocatalytic reduction of H_2O_2 using the MWCNT/PEDOT-FAD modified electrode

Different modified electrodes were examined for the electrocatalytic oxidation of AA, DA, and UA and the electrocatalytic reduction of H_2O_2 by linear sweep voltammetry. Fig. 5A shows the voltammograms of (a) MWCNT/PEDOT-FAD/GCE, (b) PEDOT-FAD/MWCNT/GCE, (c) PEDOT-FAD/GCE, (d) MWCNT/PEDOT/GCE, and (e) PEDOT/GCE examined in the presence of 2×10^{-3} M AA, 3×10^{-5} M DA and 1×10^{-5} M UA. Inset of Fig. 5A shows the anodic peak potential (E_{pa}) and net anodic current change (ΔI_{pa}) in the absence/presence of AA, DA, and UA. Although the PEDOT-FAD/MWCNT/GCE shows the high current response, it cannot provide obvious oxidation peaks and well net current contribution for these target species. The best response for target species can be found at MWCNT/PEDOT/GCE and it shows lower oxidation overpotential. Compare to ternary hybrid composites (PEDOT-FAD/MWCNT and MWCNT/PEDOT-FAD), the MWCNT/PEDOT shows efficient electrocatalytic oxidation for AA, DA, and UA. This result indicates that PEDOT and MWCNT are the active species for the electrocatalytic oxidation of AA, DA, and UA. However, the ternary hybrid composites (PEDOT-FAD/MWCNT and MWCNT/PEDOT-FAD) are still valuable to investigate because it also shows well electrocatalytic oxidation for AA, DA, and UA when compared to this series of composites. Particularly, they are designed and expected for the electrocatalytic reduction of H_2O_2 and the highest net current contribution for DA is found in MWCNT/PEDOT-FAD.

Fig. 5B shows the voltammograms of (a) MWCNT/PEDOT-FAD/GCE, (b) PEDOT-FAD/MWCNT, (c) PEDOT-FAD, (d) MWCNT/PEDOT, and (e) PEDOT/GCE examined in the presence of 5×10^{-2} M H_2O_2. Inset of Fig. 5B shows the cathodic peak potential (E_{pc}) and net cathodic current change (ΔI_{pc}) in the absence/presence of 5×10^{-2} M H_2O_2. One can see that the MWCNT/PEDOT-FAD shows higher current response although the PEDOT/GCE shows lower overpotential for the electrocatalytic reduction of H_2O_2. MWCNT/PEDOT-FAD can be the candidate due to its high net current contribution for H_2O_2.

In summary, the MWCNT/PEDOT-FAD can be a candidate due to the well recognition of AA, DA, UA, and H_2O_2 based on the obvious redox peaks and current responses.

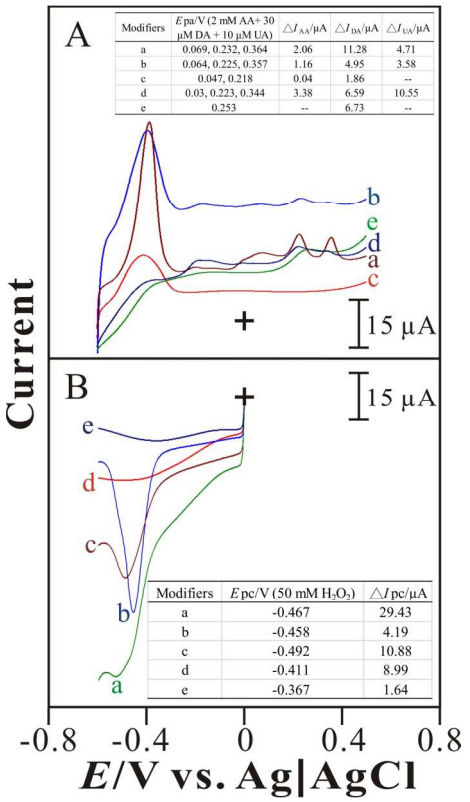

Modifiers	E pa/V (2 mM AA+ 30 μM DA + 10 μM UA)	$\triangle I_{AA}$/μA	$\triangle I_{DA}$/μA	$\triangle I_{UA}$/μA
a	0.069, 0.232, 0.364	2.06	11.28	4.71
b	0.064, 0.225, 0.357	1.16	4.95	3.58
c	0.047, 0.218	0.04	1.86	--
d	0.03, 0.223, 0.344	3.38	6.59	10.55
e	0.253	--	6.73	--

Modifiers	E pc/V (50 mM H_2O_2)	$\triangle I$ pc/μA
a	-0.467	29.43
b	-0.458	4.19
c	-0.492	10.88
d	-0.411	8.99
e	-0.367	1.64

Fig. 5. Linear sweep voltammograms of (a) MWCNT/PEDOT-FAD/GCE, (b) PEDOT-FAD/MWCNT/GCE, (c) PEDOT-FAD/GCE, (d) MWCNT/PEDOT/GCE, and (e) PEDOT/GCE examined in PBS (pH 7) containing (A) 2×10^{-3} M AA + 3×10^{-5} M DA + 1×10^{-5} M UA and (B) 5×10^{-2} M H_2O_2, respectively. Scan rate = 0.1 V s^{-1}.

3.5 Determination of AA, DA, UA, and H_2O_2 using MWCNT/PEDOT-FAD/GCE

The next attempt was taken to simultaneously determine AA, DA, and UA by MWCNT/PEDOT-FAD film modified electrode. Experiments were carried out in the range of -0.6 to 0.5 V by LSV. As can be seen in Fig. 6A, three well-defined peaks were observed at about 0.069 V, 0.232 V, and 0.364 V, corresponding to the oxidation peak of AA, DA, and UA, respectively. These well distinguished peaks allow us to simultaneously detect of AA, DA, and UA by LSV. The linear concentration range was found in 4×10^{-4} – 8×10^{-3} M, 6×10^{-6} – 7.5×10^{-5} M, and 2×10^{-6} – 4×10^{-5} M for AA, DA, and UA, respectively. The detection limit was determined in 4×10^{-4} M, 6×10^{-6} M, and 2×10^{-6} M (S/N= 3). The sensitivity was estimated in 36 μA mM^{-1} cm^{-2}, 5154 μA mM^{-1} cm^{-2}, and 14286 μA mM^{-1} cm^{-2} for AA, DA, and UA, respectively. It shows competitive performance in the literature as shown in Table 1.

The H_2O_2 determination was also taken by LSV using the MWCNT/PEDOT-FAD modified electrode (Fig. 6B). One

obvious cathodic peak is observed at -0.467 V and the peak current is directly proportional to H_2O_2 concentration. It shows linear concentration range of 5×10^{-4} – 9×10^{-3} M with the sensitivity of 52 μA mM^{-1} cm^{-2} and detection limit of 5×10^{-4} M (S/N= 3). It shows competitive sensitivity in the literature as shown in Table 2. Having above information, it would be easier to develop a multifunctional biosensor for determining AA, DA, UA, and H_2O_2 for practical fabrication.

In further consideration, the detection limit of MWCNT/PEDOT-FAD for AA and H_2O_2 is higher than that of the previously reported results in Table 1 and 2. The detection limit is not low like previous works such as helical carbon nanotubes for low detection limit of AA and noble metal composites for low detection of H_2O_2. The phenomenon might be caused by the interaction among multi-species hybrid composite. Actually, the MWCNT/PEDOT-FAD hybrid composite is mainly designed for a bifunctional biosensor for both electrocatalytic oxidation (of AA, DA, and UA) and electrocatalytic reduction (of H_2O_2). One can know that the composite can maintain most activities from their precursors. However, the composite is not able to maintain the competitive detection limit only for some target species (AA and H_2O_2). In the electrocatalytic reactions, the energy (potential) is significantly different between the electrocatalytic oxidation and reduction. For the hybrid composite, they are terminal working potentials for the electrocatalytic of AA and the electrocatalytic reduction of H_2O_2. So that, the hybrid composite might be consumed or lose competitive detection limit for AA and H_2O_2.

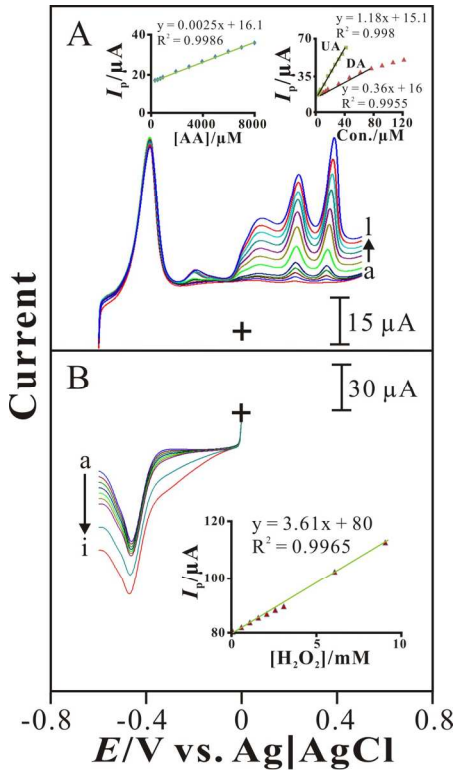

Fig. 6. Linear sweep voltammograms of MWCNT/PEDOT-FAD/GCE examined in PBS (pH 7) containing (A) AA (4×10^{-4}–8×10^{-3} M) + DA (6×10^{-6}–1.2×10^{-4} M) + UA (2×10^{-6}–4×10^{-5} M) and (B) H_2O_2 (5×10^{-4}–9×10^{-3} M), respectively. Scan rate = 0.1 V s^{-1}.

Table 1. Performance of the MWCNT/PEDOT-FAD electrode compared with other sensors.

Modifiers	Sensitivity (μA mM^{-1} cm^{-2})	Linear range (M)	Detection limit (μM)	Ref.
MWCNT/PEDOT	AA: 2.2	1×10^{-4}–2×10^{-3}	100	[26]
	DA: 17286	1×10^{-5}–3.3×10^{-4}	10	
	UA: 46857	1×10^{-5}–2.5×10^{-4}	10	
TNCs1-GCE	AA: 171	8×10^{-5}–1.4×10^{-3}	14	[42]
	DA: 57586	4×10^{-7}–6×10^{-5}	0.28	
	UA: 8643	1×10^{-5}–7×10^{-5}	1.6	
Helical carbon nanotubes	AA: 10	2.5×10^{-5}–1.1×10^{-3}	0.12	[43]
	DA: 2058	2.5×10^{-6}–1×10^{-5}	0.08	
	UA: 162	5×10^{-6}–1.8×10^{-4}	0.22	
PdNPs/graphene/ chitosan	AA: 1873	1×10^{-4}–4×10^{-3}	20	[44]
	DA: 3190, 891	5×10^{-7}–5×10^{-5}, 2×10^{-5}–2×10^{-4}	0.1	
	UA: 1057	5×10^{-7}–2×10^{-4}	0.17	
Electrochemically treated GCE	AA: 329	2.5×10^{-5}–3×10^{-4}	23.8	[45]
	DA: 7397	3×10^{-6}–3×10^{-5}	2.67	
	UA: 2761	5×10^{-6}–7×10^{-5}	4.7	
Edge plane pyrolytic graphite electrode	AA: 8.4×10^{-4}	5×10^{-8}–1.2×10^{-7}	0.08	[46]
	DA: –	–	–	
	UA: 8.7×10^{-3}	1×10^{-7}–1×10^{-3}	0.052	
1,4-naphthoquinone/ MWCNT modified basal plane pyrolytic graphite electrode	AA: 387.3	4×10^{-5}–2.8×10^{-4}	1.94	[47]
	DA: 3328305	1×10^{-8}–7×10^{-8}	0.003	
	UA: 50384	2×10^{-6}–1.4×10^{-5}	0.1	
MWCNT/ PEDOT-FAD	AA: 36	4×10^{-4}–8×10^{-3}	400	This work
	DA: 5154	6×10^{-6}–7.5×10^{-5}	6	
	UA: 14286	2×10^{-6}–4×10^{-5}	2	

Coimmobilization of different materials with specific function for electrocatalytic oxidation/reduction can be easily performed by our method. The coimmobilization of PEDOT and FAD is the electro-codeposition based on the electrostatic interaction between the positively charged PEDOT and the negatively charged FAD. It indicates that the convenient one pot process for synthesizing various materials with specific functional can be successfully performed without other binders. Although the performance is not the best one, it still provides a simple and smart method for coimmobilization of various materials with

specific functions. This kind of composite also can be further enhanced by MWCNT especially for the use of MWCNT after the electro-codeposition of PEDOT and FAD. Therefore, one simple, smart, and low-cost method is proposed for the modified artwork in the literature.

Table 2. Performance of the MWCNT/PEDOT-FAD electrode compared with other H_2O_2 sensors without horseradish peroxidase.

Modifiers	Sensitivity ($\mu A\ mM^{-1}\ cm^{-2}$)	Linear range (M)	Detection limit (μM)	Ref.
Ag/MWCNT/gold	20	5×10^{-5}–1.7×10^{-2}	0.5	[48]
Ag NP/SiO_2/graphene oxide	-	1×10^{-4}–2.6×10^{-1}	4	[49]
MnO_2/graphene oxide	38.2	5×10^{-6}–6×10^{-4}	0.8	[27]
Ag NP/attapulgite	-	1×10^{-5}–2.2×10^{-2}	2.4	[50]
Ag–MnO_2–MWCNT	82.5	5×10^{-6}–1.0×10^{-2}	1.7	[51]
MWCNT/PEDOT-FAD	52	5×10^{-4}–9×10^{-3}	500	This work

3.6 Determination of DA and UA in real samples

The application of the MWCNT/PEDOT-FAD modified electrode was investigated by direct determination of DA and UA in human urine samples. Table 3 shows the test result with very good recovery (99 ~ 101.5 %) and coefficient of variation (0.8 ~ 4.3 %). The interference from glucose, galactose, fructose, and sucrose was also studied. No oxidation peak was observed for 10 mM of these species using the MWCNT/PEDOT-FAD modified electrode. It deducts that the MWCNT/PEDOT-FAD modified electrode can be a good applicability in real samples analysis.

Table 3. Recovery of target species obtained in human urine samples using MWCNT/PEDOT-FAD hybrid composite.

Urine Sample	Added (A)/μM	Found (B)[a]/μM	Recovery[b]/%	CV[c]/%
1	DA: 6	5.99±0.25	99.50	4.3
2	DA: 12	18.85±0.45	99.04	4.1
3	DA: 18	18.10±0.40	100.49	2.3
4	UA: 20	20.10±0.60	101.53	3.6
5	UA: 40	40.00±0.60	99.79	1.5
6	UA: 60	60.05±0.05	99.97	0.8

[a] The detected amounts of target species were obtained from n = 3 analyses.
[b] Recovery (%) = (B/A)×100%.
[c] CV: coefficient of variation.

3.7 Stability study of the MWCNT/PEDOT-FAD hybrid film

Repetitive redox cycling experiments were completed to determine the extent of stability relevant to MWCNT/PEDOT-FAD modified GCE in pH 7 PBS. This investigation indicated that the peak heights of the cyclic voltammograms decreased less than 7 % after 100 continuous scan cycles with the scan rate of 100 mV s^{-1}. On the other hand, the MWCNT/PEDOT-FAD modified GCE kept its initiate activity for more than 14 days when stored at the temperature of 4℃. A decrease of 8 % was observed in current response of the electrode at the end of 14th day. And the electrocatalytic response current of MWCNT-PEDOT for H_2O_2, AA, DA, and UA can keep above 90% of original current response.

4. Conclusions

The MWCNT/PEDOT-FAD hybrid composite can be easily prepared on electrode surface by a simple method. It has been examined with good electrocatalytic properties for AA, DA, UA, and H_2O_2. It shows lower overpotential and higher current response for target species. The proposed composite can determine AA, DA, UA, and H_2O_2, expecting to be utilized to develop multifunctional biosensors.

This work was supported by the National Science Council of Taiwan (ROC).

Notes and references

Electroanalysis and Bioelectrochemistry Lab, Department of Chemical Engineering and Biotechnology, National Taipei University of Technology, No.1, Section 3, Chung-Hsiao East Road, Taipei 106, Taiwan (ROC). Fax: (886)-2-27025238; Tel: (886)-2-27017147; E-mail: smchen78@ms15.hinet.net

† Electronic Supplementary Information (ESI) available: [details of any supplementary information available should be included here]. See DOI: 10.1039/b000000x/

‡ Footnotes should appear here. These might include comments relevant to but not central to the matter under discussion, limited experimental and spectral data, and crystallographic data.

1 P. Kalimuthu and S. A. John, *Talanta*, 2010, **80**, 1686–1691.
2 S. Mahshid, C. C. Li, S. S. Mahshid, M. Askari, A. Dolati, L. X. Yang, S. L. Luo and Q. Y. Cai, *Analyst*, 2011, **136**, 2322–2329.
3 M. Mallesha, R. Manjunatha, C. Nethravathi, G. S. Suresh, M. Rajamathi, J. S. Melo and T. V. Venkatesha, *Bioelectrochemistry*, 2011, **81**, 104–108.
4 A. H. Liu, M. D. Wei, I. Honma and H. S. Zhou, *Adv. Funct. Mater.*, 2006, **16**, 371–376.
5 F. Gonon, M. Buda, R. Cespuglio, M. Jouvet and J. F. Pujol, *Nature*, 1980, **286**, 902–904.
6 Y. Liu, J. S. Huang, H. Q. Hou and T. Y. You, *Electrochem. Commun.*, 2008, **10**, 1431–1434.
7 M. Hadi and A. Rouhollahi, *Anal. Chim. Acta*, 2012, **721**, 55–60.
8 B. Habibi and M. H. Pournaghi-Azar, *Electrochim. Acta*, 2010, **55**, 5492–5498.
9 N. G. Shang, P. Papakonstantinou, M. McMullan, M. Chu, A. Stamboulis, A. Potenza, S. S. Dhesi and H. Marchetto, *Adv. Funct. Mater.*, 2008, **18**, 3506–3514.

10 C. L. Sun, H. H. Lee, J. M. Yang and C. C. Wu, *Biosens. Bioelectron.*, 2011, **26**, 3450–3455.
11 S. Y. Zhu, H. J. Li, W. X. Niu and G. B. Xu, *Biosens. Bioelectron.*, 2009, **25**, 940–943.
12 D. Zheng, J. S. Ye, L. Zhou, Y. Zhang and C. Z. Yu, *J. Electroanal. Chem.*, 2009, **625**, 82–87.
13 M. Noroozifara, M. Khorasani-Motlaghc, R. Akbaria and M. B. Parizi, *Biosens. Bioelectron.*, 2011, **28**, 56–63.
14 J. F. Ping, J. Wu, Y. X. Wang and Y. B. Ying, *Biosens. Bioelectron.*, 2012, **34**, 70–76.
15 J. Y. Qu, Y. Shen, X. H. Qu and S. J. Dong, *Chem. Commun.*, 2004, **1**, 34–35.
16 X. C. Zhao and R. T. Liu, *Environ. Int.*, 2012, **40**, 244–256.
17 K. Karnicka, K. Miecznikowski, B. Kowalewska, M. Skunik, M. Opallo, J. Rogalski, W. Schuhmann and P. J. Kulesza, *Anal. Chem.*, 2008, **80**, 7643–7648.
18 F. Patolsky, Y. Weizmann and I. Willner, *Angew. Chem. Int. Edit.*, 2004, **43**, 2113–2117.
19 M. K. Wang, F. Zhao, Y. Liu and S. J. Dong, *Biosens. Bioelectron.*, 2005, **21**, 159–166.
20 L. Ulrich, V. R. Nataliya and M. M. Vladimir, *Anal. Chemi. Acta*, 2009, **614**, 1–26.
21 J. Ouyang, C. W. Chu, F. C. Chen, Q. Xu and Y. Yang, *Adv. Funct. Mater.*, 2005, **15**, 203–208.
22 L. Groenendaal, F. Jonas, D. Freitag, H. Pielartzik and J. R. Reynolds, *Adv. Mater.*, 2000, **12**, 481–494.
23 G. Heywang and F. Jonas, *Adv. Mater.*, 1992, **4**, 116–118.
24 A. Kros, S. W. F. M. Van-Hovell, N. A. J. M. Sommerdijk and R. J. M. Nolte, *Adv. Mater.*, 2001, **13**, 1555–1557.
25 A. Kros, N. A. J. M. Sommerdijk and R. J. M. Nolte, *Sens. Actuators B*, 2005, **106**, 289–295.
26 K. C. Lin, T. H. Tsai and S. M. Chen, *Biosens. Bioelectron.*, 2010, **26**, 608–614.
27 L. Li, Z. Du, S. Liu, Q. Hao, Y. Wang, Q. Li and T. Wang, *Talanta*, 2010, **82**, 1637–1641.
28 W. Lian, L. Wang, Y. Song, H. Yuan, S. Zhao, P. Li and L. Chen, *Electrochim. Acta*, 2009, **54**, 4334–4339.
29 S. J. Guo, S. J. Dong and E. K. Wang, *Small*, 2009, **5**, 1869–1876.
30 S. J. Guo, D. Wen, S. J. Dong and E. K. Wang, *Talanta*, 2009, **77**, 1510–1517.
31 N. V. Klassen, D. Marchington and H. C. E. McGowan, *Anal. Chem.*, 1994, **66**, 2921–2925.
32 U. Pinkernell, S. Effkemann and U. Karst, *Anal. Chem.*, 1997, **69**, 3623–3627.
33 W. Lei, A. Durkop, Z. H. Lin, M. Wu and O. S. Wolfbeis, *Microchim. Acta*, 2003, **143**, 269–274.
34 Q. Wang and S. J. Dong, *Talanta*, 2000, **51**, 565–572.
35 W. Liu, D. Liu, W. T. Zheng and Q. Jiang, *J. Phys. Chem. C*, 2008, **112**, 18840–18845.
36 Q. Xu, J. J. Zhu and X. Y. Hu, *Anal. Chim. Acta*, 2007, **597**, 151–156.
37 F. L. Qu, M. H. Yang, J. H. Jiang, G. L. Shen and R. Q. Yu, *Anal. Biochem.*, 2005, **344**, 108–114.
38 Y. J. Zou, L. X. Sun and F. Xu, *Talanta*, 2007, **72**, 437–442.
39 G. Z. Zou and H. X. Ju, *Anal. Chem.*, 2004, **76**, 6871–6876.
40 K. C. Lin, Y. C. Lin and S. M. Chen, *Analyst*, 2012, **137**, 186–194.
41 K. C. Lin, C. Y. Yin and S. M. Chen, *Analyst*, 2012, **137**, 1378–1383.
42 S. Zhou, H. Shi, X. Feng, K. Xue and W. Song, *Biosens. Bioelectron.*, 2013, **42**, 163–169.
43 Zhang, D. Huang, X. Xu, G. Alemu, Y. Zhang, F. Zhan, Y. Shen and M. Wang, *Electrochim. Acta*, 2013, **91**, 261–266.
44 X. Wang, M. Wu, W. Tang, Y. Zhu, L. Wang, Q. Wang, P. He and Y. Fang, *J. Electroanal. Chem.*, 2013, **695**, 10–16.
45 Z. Temocin, *Sens. Actuators B*, 2013, **176**, 796–802.
46 R. T. Kachoosangi, C. E. Banks and R. G. Compton, *Electroanalysis*, 2006, **18**, 741–747.
47 A. X. Oliveira, S. M. Silva, F. R. F. Leite, L. T. Kubota, F. S. Damos and R. D. C. S. Luz, *Electroanalysis*, 2013, **25**, 723–731.
48 W. Zhao, H. Wang, X. Qin, X. Wang, Z. Zhao, Z. Miao, L. Chen, M. Shan, Y. Fang and Q. Chen, *Talanta*, 2009, **80**, 1029–1033.
49 W. Lu, Y. Luo, G. Chang and X. Sun, *Biosens. Bioelectron.*, 2011, **26**, 4791–4797.
50 H. Chen, Z. Zhang, D. Cai, S. Zhang, B. Zhang, J. Tang and Z. Wu, *Talanta*, 2011, **86**, 266–270.
51 Y. Han, J. Zheng and S. Dong, *Electrochim. Acta*, 2013, **90**, 35–43.